Journal of Magnetism and Magnetic Materials 429 (2017) 299–304

Contents lists available at ScienceDirect

Journal of Magnetism and Magnetic Materials

journal homepage: www.elsevier.com/locate/jmmm

Atomic layer deposition of titanium oxide films on As-synthesized magnetic Ni particles: Magnetic and safety properties

Peep Uudeküll[a,*], Jekaterina Kozlova[a], Hugo Mändar[a], Joosep Link[c], Mariliis Sihtmäe[b], Sandra Käosaar[b,d], Irina Blinova[b], Kaja Kasemets[b], Anne Kahru[b], Raivo Stern[c], Tanel Tätte[a], Kaupo Kukli[a,e], Aile Tamm[a]

[a] Institute of Physics, University of Tartu, W. Ostwaldi Str.1, 50411 Tartu, Estonia
[b] Laboratory of Environmental Toxicology, National Institute of Chemical Physics and Biophysics, Akadeemia tee 23, 12618 Tallinn, Estonia
[c] Laboratory of Chemical Physics, National Institute of Chemical Physics and Biophysics, Akadeemia tee 23, 12618 Tallinn, Estonia
[d] Faculty of Chemical and Materials Technology, Tallinn University of Technology, Ehitajate tee 5, 19086 Tallinn, Estonia
[e] University of Helsinki, Department of Chemistry, P.O. Box 55, FI-00014 Helsinki, Finland

ARTICLE INFO

Keywords:
Nickel mesoparticles
Atomic layer deposition (ALD)
Titanium dioxide coatings
Magnetical characterization
Safety

ABSTRACT

Spherical nickel particles with size in the range of 100–400 nm were synthesized by non-aqueous liquid phase benzyl alcohol method. Being developed for magnetically guided biomedical applications, the particles were coated by conformal and antimicrobial thin titanium oxide films by atomic layer deposition. The particles retained their size and crystal structure after the deposition of oxide films. The sensitivity of the coated particles to external magnetic fields was increased compared to that of the uncoated powder. Preliminary toxicological investigations on microbial cells and small aquatic crustaceans revealed non-toxic nature of the synthesized particles.

1. Introduction

During the past few decades, the use of fine magnetic particles in biomedical applications has gone through rapid growth. However, uniform size micro- and mesoscale particles have attracted far less attention than ultrafine particles as scientists are striving for new nano-applications. In one of the earliest works by Widder et al. [1] in late 1970s, mesoscale (nanometers to microns) magnetic particles were used for magnetic delivery of chemotherapy compounds to a specific site *in vivo*. In 1990, Miltenyi et al. [2] suggested a magnetic cell separation process in which a specially designed steel microfiber filled with fluorescently labeled magnetic microparticles was used in a separation column in order to isolate a specific cell population from a heterogeneous sample. A decade later, Mah et al. [3] were the first in the field of gene transfection using magnetic microparticles to deliver genes into cells by linking a viral vector to the particles.

The amount of research done has been growing ever since. The development of applications based on the most basic principle of magnetism, i.e. magnetic interaction at a distance, can revolutionize fields such as cancer and gene therapy, tissue engineering, developmental biology etc. For example, transition metal mesoparticles will be more used in a wide range of biomedical applications, such as magnetic cell separation, drug targeting, magnetic fluid hyperthermia and other magnetism-based health applications [4].

Out of the array of transition metals, nickel is one of the most important magnetic materials with properties, that make it suitable for several previously mentioned applications [5,6]. However, several magnetic particles (including Ni) possess danger to living organisms not only due to toxic properties, but also due to other factors, such as particle aggregation [7]. These circumstances can possess catastrophic consequences, as clustered particles may block blood flow if applied *in vivo*. However, by coating the particles with biocompatible substances (e.g. TiO_2), it is possible to increase the safety of the particles. This kind of safer-by-design approach has recently been shown by Gass et al. [8], who applied TiO_2 coating to various nanomaterials (CeO_2, Fe_2O_3, ZnO, Ag) and observed significantly reduced toxicological effects compared to uncoated particles.

A surface functionalization method, whose potential is underused in the field of biomedicine, is atomic layer deposition (ALD). ALD belongs to a group of chemical vapour deposition (CVD) layer-by-layer techniques. It relies on self-limiting surface reactions of gases that are alternately introduced into and purged out of the reaction chamber, and consequently, it is possible to achieve conformal deposition with atomic precision on various nanostructured architectures with large

* Corresponding author.
E-mail address: peep.uudekull@ut.ee (P. Uudeküll).

http://dx.doi.org/10.1016/j.jmmm.2017.01.045
Received 28 November 2016; Accepted 13 January 2017
Available online 14 January 2017
0304-8853/

aspect ratios [9,10]. Therefore, the alteration of the surface properties of the particles generally does not affect the bulk properties of the cores.

When targeting biomedical applications, one can propose using TiO_2 as the shell material due to its chemical and mechanical stability important for corrosion protection combined with photocatalytical properties for antimicrobial purpose [11,12].

Processes that can be used for fabricating Ni core mesoparticles include chemical reduction [13], sol–gel deposition [14], combustion reaction [6], etc. Among them, liquid phase methods have been widely applied because of their relative simplicity, flexibility and better control over the size of forming particles. The benzyl alcohol method is a widely applicable non-aqueous liquid phase approach for the synthesis of crystalline metal (oxide) structures in solution and at low temperatures - this solvothermal process includes the reaction of metal precursor with the benzyl alcohol as a liquid medium at temperatures in the range of 50–250 °C [15]. Owing to surfactant free fabrication, high crystallinity of the particles, dual role of the solvent, size controllability, etc., it has several advantages over other methods [16–18].

In the present study nickel mesoscale particles (100–400 nm) were synthesized using the benzyl alcohol method. The synthesized particles were subsequently coated with a thin TiO_2 layer by ALD. For ALD of TiO_2 on Ni particles, a well-known and earlier described reliable ALD process based on the application of titanium tetrachloride and water [19,20] was exploited. The size, morphology, magnetic properties and the toxicity of the coated and uncoated Ni mesoparticles to bacteria *Vibrio fischeri*, yeast *Saccharomyces cerevisiae* and freshwater crustacean *Thamnocephalus platyurus* were evaluated. The magnetic behavior of the particles was evaluated by vibrating sample magnetometer in order to explore the possibility to rapidly magnetize and demagnetize the metal sensing cores as well as the possible promotional or destructive effects of the oxide coatings on the metal.

2. Experimental details

2.1. Synthesis of particles

1.0 g of nickel(II)acetylacetonate (Sigma-Aldrich, 95%), was added to 20 mL of benzyl alcohol (Sigma-Aldrich, 99%) in a 100 mL round bottom flask, which was sealed and placed on a magnetic stirrer for 24 h. After obtaining a homogeneous solution, the mixture was heated on an oil bath at 180 °C for 24 h. The resulting black precipitate was filtered and repeatedly rinsed in pure acetone, in order to remove the chemicals adsorbed on the surface of the particles. The precipitate was dried in air at room temperature (25 °C), collected in the form of powder, and divided into two sets of samples. One of them was coated with TiO_2 film by ALD, after which both samples were characterized as described in 2.3.

2.2. Coating the particles via atomic layer deposition

The TiO_2 film on nickel powder was deposited in a flow-type in-house built hot-wall ALD reactor [20] using $TiCl_4$ (Sigma-Aldrich, 99.99%) and H_2O as precursors. N_2 was used as a carrier gas while the reactor pressure ranged from 195 to 260 Pa. At first, thin amorphous nucleation layers of TiO_2 were grown by applying 10 ALD cycles at 150 °C followed by 300 ALD cycles at 300 °C. The cycle times were 30–30–0–0 s at 150 °C and 10–20-2–10 s at 300 °C for the $TiCl_4$ pulse, first purge, H_2O pulse and the second purge period, respectively. The two-temperature process was applied in order to start the deposition at low temperature, i.e. using, presumably, a less destructive growth mode, which can also provide higher nucleation density due to the preferred growth of amorphous, disordered material. The deposition of TiO_2 was then completed by the growth at higher temperature providing more intense crystal growth and higher chemical purity [21].

2.3. Characterization

The surface morphology and thicknesses of TiO_2 films were evaluated by high-resolution scanning electron microscope (HRSEM) Helios NanoLab 600 (FEI) equipped with focused ion beam (FIB) module. The film thicknesses were determined from SEM images taken from sample cross-sections prepared by FIB or with spectroscopic ellipsometry (SE) on reference planar substrates. Compositions of coated and uncoated particles were measured by an energy dispersive X-ray spectrometer (EDS) INCA Energy 350 (Oxford Instruments). Structural characterization was performed by X-ray diffraction (XRD) analysis (Rigaku SmartLab), using CuKα radiation with diffraction angle (2θ) ranging from 15°–80°, and by Raman spectroscopy using a Renishaw *in via* micro-Raman spectrometer with the incident argon-ion laser beam wavelength of 514 nm and spectral resolution of 1.5 cm^{-1}. The magnetic measurements were performed on the 14 T vibrating sample magnetometer – physical property measurement system (VSM-PPMS, Quantum Design). Hysteresis measurements were performed by scanning the magnetic field from -1.6×10^6 to $+1.6\times10^6$ A/m at room temperature.

2.4. Toxicity testing

2.4.1. Preparation of particles suspensions

Stock solution of uncoated and TiO_2-coated Ni particles (5 g Ni/L) were prepared in deionized (DI) water (pH 5.6 ± 0.1) (Milli-Q, Millipore) and the suspensions were homogenized using ultrasonic probe (Branson Digital Sonifier, USA) for 4 min at 40 W immediately after suspension preparation. Soluble nickel salt, $NiCl_2{\cdot}6H_2O$ (Merck) (5 g Ni/L in DI), was used as the ionic control for Ni particles and $CuSO_4$ (Alfa Aesar) (5 g Cu/L in DI) was used as the standard positive control for the selected toxicity tests.

2.4.2. Toxicity evaluation using naturally luminescent bacteria Vibrio fischeri

The bioluminescence inhibition assay with luminescent bacteria *Vibrio fischeri* was used for toxicity evaluation of coated and uncoated Ni-particles. In this assay, the luminescence of the bacteria decreases in concentration-dependent manner upon exposure to toxic chemicals [22]. The 30-min kinetic bioluminescence inhibition assay (a Flash-test) was performed as described in Mortimer *et al.* following the standard protocol (ISO 21338, 2010) [23,24]. The assay was performed at room temperature (~20 °C) on 96-well microplates using a Microplate Luminometer Orion II (Berthold Detection Systems, Pforzheim, Germany), controlled by Simplicity Version 4.2 Software. Reconstituted *V. fischeri* Reagent (Aboatox, Turku, Finland) was used as the test bacteria suspension and 2% NaCl as a diluent and as a negative control. Each test was performed in 5–7 replicates using exponential dilutions. Ni compounds were tested at nominal concentration range of 0.075—500 mg Ni/L.

The test results were expressed as EC_{50} values (the nominal concentration of a compound reducing the bioluminescence by 50%) determined from the concentration-effect curves by the application of the log-normal model using REGTOX software for Microtox Excel™ (MS Excel macro REGTOX EV7.0.5.xls).

2.4.3. Toxicity evaluation using yeast Saccharomyces cerevisiae

A 'spot' assay format described in Suppi et al. was used [25]. In this test yeast cells were exposed to different concentrations of the chemical of interest in DI water for 24 h and after that the colony-forming ability of the exposed and unexposed (control) cells on toxicant-free agarized growth medium was evaluated. As a result, a minimum biocidal concentration (MBC) of the chemical was determined.

S. cerevisiae BY4741 (EUROSCARF, Institute of Microbiology, University of Frankfurt, Germany) was used as a test organism. Briefly, 75 μL of yeast cells in DI water (~10^7 viable cells/mL) were

exposed 1:1 to the test chemicals on 96-well microplates in DI water (total volume 150 µL per well). DI water without test chemicals inoculated with the yeast cells served as the control. Ni compounds were tested from 0.01—1000 mg Ni/L (ten-fold dilutions). Test plates were incubated at 25 °C for 24 h without shaking in the dark. After 24-h exposure, 5 µL of test culture from each microplate well was transferred as a spot onto toxicant-free yeast extract-peptone-dextrose (YPD) agar plates and incubated for 72 h at 30 °C. Minimum biocidal concentration (MBC) of the tested Ni compounds and $CuSO_4$ (a positive control) was determined as the lowest tested nominal concentration which completely inhibited the outgrowth of the exposed cells, i.e. formation of visible colonies on toxicant-free agar medium.

2.4.4. Toxicity evaluation using freshwater crustaceans Thamnocephalus platyurus

T. platyurus was used as a test organism and the test was performed as described in Standard Operational Procedures of Thamnotoxkit F™ (1995) [26]. Briefly, *T. platyurus* larvae obtained by the hatching of cysts were exposed to different concentrations of chemical of interest for 24 h at 25 °C in the dark and the mortality was used as the toxicity endpoint. The tests were performed in triplicate. The test results were expressed as LC_{50} values (the nominal concentration of a compound causing the death of 50% of the studied organisms) and were calculated using MS Excel macro REGTOX software (see above).

3. Results and discussion

Fig. 1 represents the SEM images of the uncoated and coated Ni particles and shows that both of the particles were almost spherical. It has been observed earlier that the benzyl alcohol based method provides spherical morphology of the particles [27]. Herewith the size of the particles synthesized in our study varied from 100 to 400 nm and the average size of the particle was close to 300 nm (Fig. 1A, inset). The particles appeared to be somewhat agglomerated, probably in order to minimize the total surface energy of the system [28], driven by their large surface-to-volume ratio and strong magnetic forces. The size and shape of TiO_2-coated Ni particles (Fig. 1B) were practically identical to their uncoated counterparts (Fig. 1A), as ALD enabled uniform deposition of 10 nm TiO_2 layer (Fig. 1C). One can see that the TiO_2, distinct as the thin dark layer between conducting Ni particles and Pt coating, has uniformly covered the particles in the FIB-SEM image. The layer grown by ALD added about 20 nm to the total diameter of the particles.

Composition analysis of the Ni particles did not show considerable effect of oxygen on the composition (surface) of the particles, i.e. the oxidation of Ni (Table 1). The EDS analysis carried out on the particles coated with the TiO_2 film revealed 3.7 wt% of residual chlorine. The results obtained demonstrated that, although the substrate temperature was low and the aspect ratio for the powder as the substrate was high, chlorine was quite efficiently removed from the film surface during the deposition process.

XRD patterns of the coated and uncoated Ni samples are presented in Fig. 2. Both patterns show three strong reflections at 2θ values of 44.45, 51.8 and 76.36° which can be indexed as 111, 200 and 220 of cubic (fcc) nickel (JCPDS card 4–0850). XRD crystallite size of Ni particles was 29 nm calculated from the integral width of the reflection 111 using the Scherrer formula. This crystallite size, compared to particle size of 300 nm (from SEM), indicates that Ni particles were mainly polycrystalline. The thin titanium dioxide coating on powder particles in sample (b) was recognized and identified by a weak and broad (XRD crystallite size 7 nm) reflection at 25.2° matching with the strongest reflection 101 of anatase (JCPDS card 65–5714).

In the Raman spectra taken from the uncoated Ni particles the peak at 1080 cm^{-1} appeared, typical for Ni nanoparticles (Fig. 3) and after the growth of TiO_2 film on the particles, anatase was recognized with the characteristic peak at 144 cm^{-1} [29].

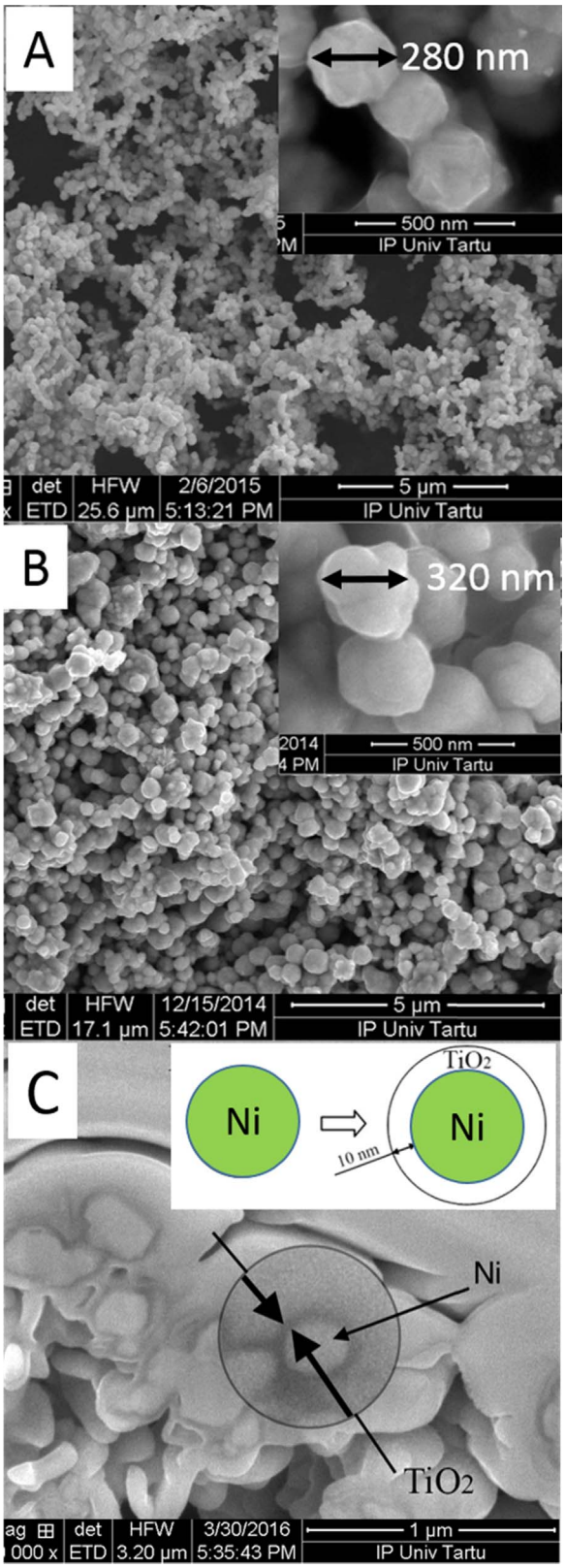

Fig. 1. SEM image of the uncoated (A) and TiO_2-coated (B) Ni particles and the SEM-FIB image of TiO_2-coated Ni particles (Fig. C). The particles (Fig. C) were coated with platinum (conductive material on isolator) to get better resolution on SEM image of thin TiO_2 films on coated Ni particles.

It has been stated that nickel nanoparticles, in particular Ni nanowires, are not Raman active [30] and the Raman studies have

Table 1
The EDX analysis of Ni particles (uncoated) and TiO_2-coated Ni particles.

Element	C	O	Ni	Ti	Cl	Total
Ni	3,4%	0,7%	95,9%	0%	0%	100%
Ni + TiO_2	2.2%	6,7%	78,4%	9,0%	3,7%	100%

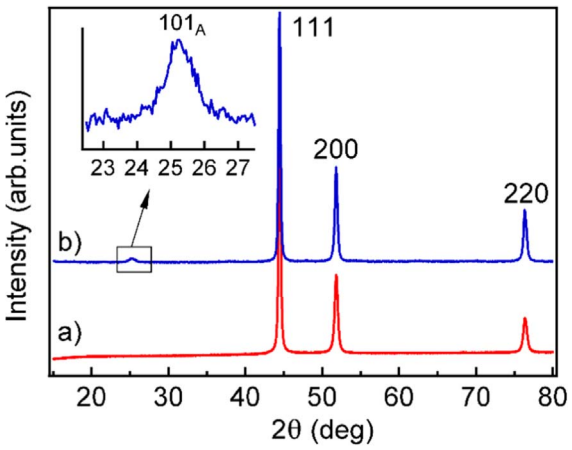

Fig. 2. X-ray diffraction patterns of uncoated a) and TiO_2-coated b) Ni samples. Miller indices of corresponding lattice planes are shown at peak top position.

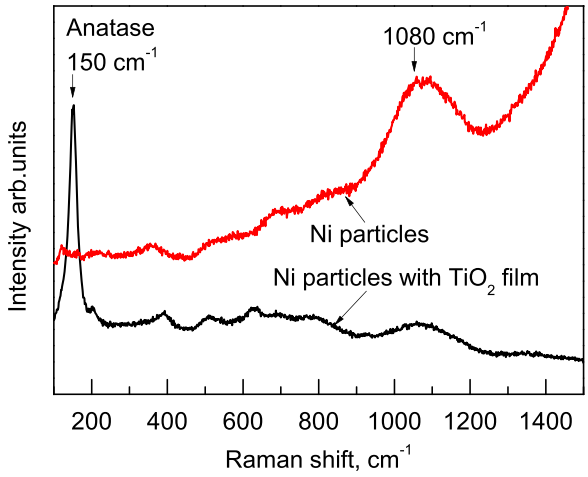

Fig. 3. The strongest reflection of anatase also detected is magnified in the inset (A). Room-temperature micro-Raman spectra of Ni particles and coated ones with TiO_2 films in Anatase phase (B). Raman peaks recognized are denoted by labels (B).

indeed mostly been carried out either on oxidized [31,32], or functionalized Ni, e.g. nickel-carbon core-shell composites [33]. Thus, decided on the basis of the Raman spectra in the present study, one can also not exclude partial oxidation of nickel particles.

The magnetization curves (Fig. 4) of the samples clearly demonstrate saturation regime in the magnetization-field curves. The curves are also characterized by rather weak coercive forces, and, consequently, narrow hysteresis loops. This is characteristic of soft magnetic materials and may be regarded as a prospective property for a magnetic sensor material that is to be quickly magnetized and demagnetized. The saturation magnetization M_s of coated and uncoated Ni particles measured at room temperature was 51 and 53 A × m^2/kg respectively, which indicated that the deposition of thin TiO_2 film has increased the M_s by 4%. For reference, the M_s of bulk nickel is 55 A×m^2/kg [34]. For further comparison, for Ni nanocrystals embedded in an alumina matrix [35], the M_s measured has been slightly higher that 67 A×m^2/kg even though the particles were smaller by an order of magnitude, compared to those synthesized in the present study. However, the

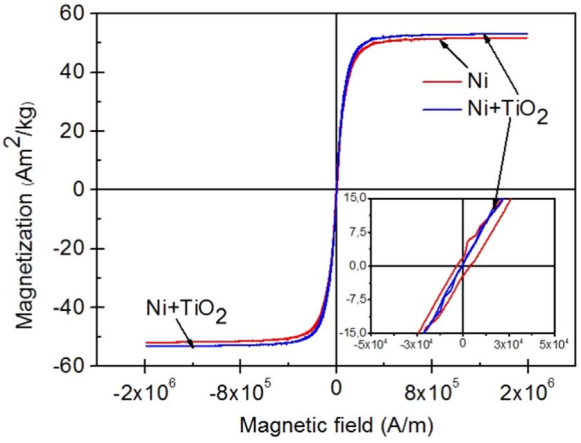

Fig. 4. Magnetization curve of the nickel compound (red) and its ALD coated counterpart (blue). (For interpretation of the references to color in this figure legend, the reader is referred to the web version of this article).

coercivity (H_c) was nearly immeasurable. In the present study, H_c for the TiO_2-coated Ni was only 238 A/m while the uncoated counterpart possessed H_c of 3580 A/m. So it can be stated that the TiO_2-coated Ni particles could demonstrate better magnetic sensor properties than the uncoated particles.

All substances on the European market manufactured or imported in quantities of 1 t or more per year have to be evaluated for their hazardous effects to humans and environment. This is in accordance with the European Union (EU) chemical safety regulations on Registration, Evaluation, Authorization and Restriction of Chemicals (REACH; EC, 2006) [36], and Classification, Labeling and Packaging (CLP) of substances and mixtures (EC, 2008) [37]. For that a number of standardised toxicity tests are developed and have to be applied, e.g. the basic ecotoxicological information requirements include short-term toxicity testing on invertebrates (preferred species *Daphnia*; OECD 202, 2004) [38] and growth inhibition study on aquatic plants (algae preferred; OECD 201, 2011) [39]. The preliminary toxicity screening on (eco)toxicologial effects of uncoated and TiO_2-coated Ni particles were conducted with two different groups of unicellular organisms, bacteria (a prokaryotic organisms) and yeast (a eukaryotic organism). In addition, a particle-ingesting aquatic crustacean was selected as a representative consumer at the food-web level (Table 2). The results of toxicity testing were expressed as EC_{50}/LC_{50}/MBC values based on nominal exposure concentrations. For the hazard ranking of the tested particles following criteria were applied: EC_{50}/LC_{50}/MBC value < 1 mg/l very toxic; 1–10 mg/l = toxic; 10–100 mg/l = harmful; > 100 mg/L = not classified/not harmful [40].

Since bacteria are ubiquitous organisms in soil and water, being important link in the terrestrial and aquatic food-webs as decomposers, *Vibrio fischeri* bioluminescence inhibition assay was chosen. No inhibition of luminescence by Ni uncoated and TiO_2-coated particles was observed even at 500 mg Ni/L, i.e. Ni particles could be considered as non-hazardous according to the used bacterial test. The latter was also supported by the parallel analysis of the toxicity of respective soluble Ni-salt; the 30-min EC_{50} value for $NiCl_2$ was 408.7 mg Ni/L (Table 2). The 30-min EC_{50} values at 15 °C (optimal temperature for bacteria *Vibrio fischeri*) obtained by other authors for $NiCl_2$ (as for Ni) were in the range of 42.2–208.7 mg/L [41,42] and are 2–10 fold lower compared to the results from the current study at 20 °C (as 15 °C is not compatible with the conventional plate luminometers). However, this difference can be explained by the different testing conditions used (e.g., 15 °C *vs* 20 °C).

Saccharomyces cerevisiae viability (colony-forming-ability) inhibition assay is not conventional standard test for the environmental hazard evaluation. In this study the yeast cells were studied as a model for the eukaryotic cell as *S. cerevisiae* cells have quite similar cellular

Table 2
Toxicity of uncoated and TiO_2-coated Ni particles to bacteria *Vibrio fischeri*, yeast *Saccharomyces cerevisiae* BY4741 and crustaceans *Thamnocephalus platyurus*.

Test species	Bacterium *V. fischeri*	Yeast *S. cerevisiae*	Freshwater crustacean *T. platyurus*
Characterization of the test species	Prokaryotic unicellular organisms, a priori particle'proof'	Eukaryotic unicellular organisms. particles endocytosis activity	Multicellular invertebrate; particle-ingesting organisms
Toxicity (mg metal/L) and toxicity endpoint)	30-min EC_{50}[a] [mg/L] (inhibition of luminescence)	24-h MBC[b] [mg/L] (colony forming ability)	24-h LC_{50}[c] [mg/L] (mortality)
CHEMICALS TESTED			
TiO_2-coated Ni particles	> 500	> 1000	521
Uncoated Ni particles	> 500	> 1000	662
$NiCl_2 \times 6H_2O$ (ionic control	409	> 1000	5.50[d]
$CuSO_4$ (positive control for the test validation)	0.16	10.0	0.012

[a] EC_{50} – half-effective concentration;
[b] MBC - minimum biocidal concentration - the lowest tested concentration that completely inhibited the visible growth/colony formation of yeast on the agarized growth medium after 24-h exposure to the tested compounds.
[c] LC_{50} – half-lethal concentration. All concentrations are nominal. Tentative hazard ranking: ≤1 mg/L, very toxic; > 1–10 mg/L, toxic; > 100 mg/L, not classified/not harmful [35].

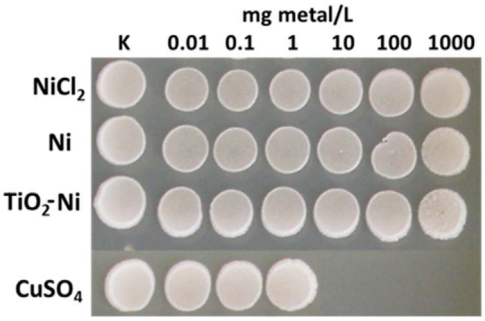

Fig. 5. Colonies (visible as 'spots') of *yeast Saccharomyces cerevisiae* on agarised growth medium. Ni-compounds showed no effect of colony forming potential even at 1000 mg Ni/L. Absence of growth (spots) in case of Cu-ions (a positive control) at exposure concentrations higher than 1 mg Cu/L indicates toxic effects.

structure and particles endocytosis ability as mammalian cells and also as a fungal model as the yeast cells different from mammalian cells have a thick outer mannan-β-glucan-chitin cell wall [43,44].

We have previously demonstrated that algae and crustaceans are the most sensitive and thus probably the most vulnerable organism groups in aquatic exposure to nanomaterials [40]. According to the data obtained in the present study, both uncoated and TiO_2-coated Ni particles, were not toxic to *T. platyurus* (24-h EC_{50} > 500 mg Ni/L). However, soluble Ni-salt ($NiCl_2$) proved to be harmful to *T. platyurus* (24-h EC_{50}=5.5 mg Ni/L) (Table 2) indicating that the Ni-particles may cause toxicity to crustaceans if the conditions support their solubilisation (i.e. shedding of Ni-ions).

Results showed that the uncoated and TiO_2-coated Ni particles and Ni-ions did not affect adversely the viability (colony forming ability) of the yeast *S. cerevisiae* cells up to 1000 mg Ni/L (MBC > 1000 mg Ni/L) (Table 2, Fig. 5).

Summing up, short-term toxicity screening showed that both uncoated as well TiO_2-coated Ni-particles can be classified as nontoxic substances to bacteria, yeast and crustaceans.

4. Summary

Nickel particles were synthesized via benzyl alcohol method. The reaction resulted in spherical shape particles, predominantly in the size range of 100–400 nm. The surface of the particles was successfully coated with 10 nm thick TiO_2 film in anatase phase by ALD method. Magnetic measurements indicated weak hysteresis in the case of uncoated Ni particles compared to the even smaller coercivity in their coated counterpart. Saturation magnetization can be recorded in both coated and uncoated cases. Uncoated and TiO_2-coated Ni particles proved to be not harmful according to the bioassays used (bacteria, yeasts, crustaceans) pointing to the non-toxic nature of the synthesized particles and indicating a promising base for future applications. Since the nickel particles coated with thin titanium oxide layers responded to the variations of external magnetic fields, rapidly magnetizing and demagnetizing, as measured and reported, one can consider certain potential for the application of the materials studied in the biocompatible sensorics. Therefore, it is necessary to further analyze biocompatibility (i.e. to conduct assays on mammalian cells *in vitro*), surface functionalization and magnetic properties, which are the biggest challenges in complex biological environments.

Acknowledgements

The work was supported by Estonian Research Council Grants IUT2-24, IUT23-5, ETF9001, ETF9292, PUT210, PUT170 and by the European Regional Development Fund projects TK134 „Emerging orders in quantum and nanomaterials". The authors are grateful to Dr. Liis Seinberg (NICBP) for fruitful discussions.

References

[1] K.J. Widder, A.E. Senyei, G.D. Scarpelli, Magnetic microspheres: a model system of site specific drug delivery in vivo, Proc. Soc. Exp. Biol. Med. 158 (1978) 141–146. http://dx.doi.org/10.1007/978-1-4613-2745-5_15.
[2] S. Miltenyi, W. Muller, W. Weichel, A. Radbruch, High gradient magnetic cell separation with MACS, Cytometry 11 (1990) 231–238. http://dx.doi.org/10.1002/cyto.990110203.
[3] C. Mah, T.J. Fraites, I. Zolotukhin, S. Song, T.R. Flotte, J. Dobson, C. Batich, B.J. Byrne, Improved method of recombinant AAV2 delivery for systemic targeted gene therapy, Mol. Ther. 6 (2002) 106–112. http://dx.doi.org/10.1006/mthe.2001.0636.
[4] B. Kozissnik, J. Dobson, Biomedical applications of mesoscale magnetic particles, MRS Bull. 38 (2013) 927–932. http://dx.doi.org/10.1557/mrs.2013.257.
[5] S.-H. Wu, D.-H. Chen, Synthesis and characterization of nickel nanoparticles by hydrazine reduction in ethylene glycol, J. Colloid Interface Sci. 259 (2003) 282–286. http://dx.doi.org/10.1016/S0021-9797(02)00135-2.
[6] N.M. Deraz, Formation and magnetic properties of metallic nickel nano- particles, Int. J. Electrochem. Sci. 7 (2012) 4608–4616.
[7] A.P. Romio, H.H. Rodrigues, A. Peres, A.D.C. Viegas, E. Kobitskaya, U. Ziener, K. Landfester, C. Sayer, P.H.H. Araújo, Encapsulation of magnetic nickel nanoparticles via inverse miniemulsion polymerization, J. Appl. Polym. Sci. 129 (2013) 1426–1433. http://dx.doi.org/10.1002/app.38840.
[8] S. Gass, J.M. Cohen, G. Pyrgiotakis, G.A. Sotiriou, S.E. Pratsinis, P. Demokritou, Safer formulation concept for flame-generated engineered nanomaterials, ACS Sustain. Chem. Eng. 1 (2013) 843–857. http://dx.doi.org/10.1021/sc300152f.
[9] M. Smietana, M. Koba, E. Brzozowska, K. Krogulski, J. Nakonieczny, L. Wachnicki, P. Mikulic, M. Godlewski, W. J. Bock, Label-Free Sensitivity of Long-period Gratings Enhanced by Atomic Layer Deposited TiO2 Nano-overlays, vol. 23, 2015, pp. 3530–3536. ⟨http://doi.org/10.1364/OE.23.008441⟩
[10] Y. Zhang, C. Guerra-nun, I. Utke, J. Michler, M.D. Rossell, R. Erni, Understanding and controlling nucleation and growth of TiO_2 deposited on multiwalled carbon nanotubes by atomic layer deposition, J. Phys. Chem. C 119 (2015) 3379–3387. http://dx.doi.org/10.1021/jp511004h.
[11] S.D. Standridge, G.C. Schatz, J.T. Hupp, Toward plasmonic solar cells: protection of silver nanoparticles via atomic layer deposition of TiO_2, Langmuir 25 (2009) 2596–2600. http://dx.doi.org/10.1021/la900113e.
[12] M. Vähä-Nissi, M. Pitkänen, E. Salo, E. Kenttä, A. Tanskanen, T. Sajavaara, M. Putkonen, J. Sievänen, A. Sneck, M. Rättö, M. Karppinen, A. Harlina, Antibacterial and barrier properties of oriented polymer films with ZnO thin films applied with atomic layer deposition at low temperatures, Thin Solid Films 562 (2014) 331–337. http://dx.doi.org/10.1016/j.tsf.2014.03.068.

[13] Y.L. Hou, S. Gao, Solvothermal reduction synthesis and magnetic properties of polymer protected iron and nickel nanocrystals, J. Alloy. Compd. 365 (2004) 112–116. http://dx.doi.org/10.1016/S0925-8388(03)00651-0.
[14] J. Gong, L.L. Wang, Y. Liu, J.H. Yang, Z.G. Zong, Structural and magnetic properties of hcp and fcc Ni nanoparticles, J. Alloy. Compd. 457 (2008) 6–9. http://dx.doi.org/10.1016/j.jallcom.2007.02.124.
[15] N. Pinna, M. Karmaoui, M.G. Willinger, The "benzyl alcohol route": an elegant approach towards doped and multimetal oxide nanocrystals, J. Sol.-Gel Sci. Technol. 57 (2011) 323–329. http://dx.doi.org/10.1007/s10971-009-2111-2.
[16] I. Djerdj, D. Arčon, Z. Jagličić, M. Niederberger, Nonaqueous synthesis of metal oxide nanoparticles: short review and doped titanium dioxide as case study for the preparation of transition metal-doped oxide nanoparticles, J. Solid State Chem. 181 (2008) 1571–1581. http://dx.doi.org/10.1016/j.jssc.2008.04.016.
[17] N. Pinna, M. Niederberger, Surfactant-free nonaqueous synthesis of metal oxide nanostructures, Angew. Chem. - Int. Ed. 47 (2008) 5292–5304. http://dx.doi.org/10.1002/anie.200704541.
[18] P. Rauwel, E. Rauwel, C. Persson, M.F. Sunding, A. Galeckas, One step synthesis of pure cubic and monoclinic HfO_2 nanoparticles: correlating the structure to the electronic properties of the two polymorphs, J. Appl. Phys. 112 (2012) 1–9. http://dx.doi.org/10.1063/1.4766272.
[19] J. Aarik, A. Aidla, H. Mändar, T. Uustare, Atomic layer deposition of titanium dioxide from $TiCl_4$ and H_2O: investigation of growth mechanism, Appl. Surf. Sci. 172 (2001) 148–158. http://dx.doi.org/10.1016/S0169-4332(00)00842-4.
[20] T. Arroval, L. Aarik, R. Rammula, V. Kruusla, J. Aarik, Effect of substrate-enhanced and inhibited growth on atomic layer deposition and properties of aluminum–titanium oxide films, Thin Solid Films 600 (2016) 119–125. http://dx.doi.org/10.1016/j.tsf.2016.01.024.
[21] A. Tamm, A.-L. Peikolainen, J. Kozlova, H. Mändar, A. Aidla, R. Rammula, L. Aarik, K. Roosalu, J. Lu, L. Hultman, M. Koel, K. Kukli, J. Aarik, Atomic layer deposition of high-k dielectrics on carbon nanoparticles, Thin Solid Films 538 (2013) 16–20. http://dx.doi.org/10.1016/j.tsf.2012.09.071.
[22] A.Kahru, *In vitro* toxicity testing using marine luminescent bacteria (*Photobacterium phosphoreum*) – The BIOTOXTM test, ATLA. Alternatives to Laboratory Animals, vol. 21(2), pp. 210–215
[23] M. Mortimer, K. Kasemets, M. Heinlaan, I. Kurvet, A. Kahru, High throughput kinetic *Vibrio fischeri* bioluminescence inhibition assay for study of toxic effects of nanoparticles, Toxicol. Vitr. 22 (2008) 1412–1417. http://dx.doi.org/10.1016/j.tiv.2008.02.011.
[24] ISO 21338, Water quality - Kinetic determination of the inhibitory effects of sediment, other solids and coloured samples on the light emission of *Vibrio fischeri* (kinetic luminescent bacteria test), International Organization for Standardization, Geneva, Switzerland, 2010.
[25] S. Suppi, K. Kasemets, A. Ivask, K. Kunnis-Beres, M. Sihtmäe, I. Kurvet, V. Aruoja, A. Kahru, A novel method for comparison of biocidal properties of nanomaterials to bacteria, yeasts and algae, J. Hazard. Mater. 286 (2015) 75–84. http://dx.doi.org/10.1016/j.jhazmat.2014.12.027.
[26] Thamnotoxkit F™, Crustacean toxicity screening test for freshwater. Standard Operational Procedure. MicroBioTest Inc, Deinze, 1995, p 23.
[27] Y.B. Mollamahaleh, D. Hosseini, M. Mazaheri, S.K. Sadrnezhaad, Surfactant-free production of Ni-based nanostructures, Mater. Sci. Appl. 02 (2011) 444–452. http://dx.doi.org/10.4236/msa.2011.25059.
[28] K.S. Rao, T. Balaji, Y. Lingappa, M.R.P. Reddy, T.L. Prakash, Chemical synthesis and magnetic properties of HCP and FCC nickel nanoparticles, Ph. Transit. 85 (2012) 235–243. http://dx.doi.org/10.1080/01411594.2011.608255.
[29] I.M. Clegg, N.J. Everall, B. King, H. Melvin, C. Norton, On-line analysis using Raman spectroscopy for process control during the manufacture titanium dioxide, Appl. Spectrosc. 55 (2001) 1138–1150. http://dx.doi.org/10.1366/0003702011953388.
[30] G. Sauer, G. Brehm, S. Schneider, H. Graener, G. Seifert, K. Nielsch, J. Choi, P. Göring, U. Gösele, P. Miclea, R.B. Wehrspohn, Surface-enhanced Raman spectroscopy employing monodisperse nickel nanowire arrays, Appl. Phys. Lett. 88 (2006) 023106. http://dx.doi.org/10.1063/1.2162682.
[31] N. Mironova-Ulmane, A. Kuzmin, I. Sildos, M. Pärs, Polarisation dependent Raman study of single-crystal nickel oxide, Cent. Eur. J. Phys. 9 (2011) 1096–1099. http://dx.doi.org/10.2478/s11534-010-0130-9.
[32] L. De Los Santos Valladares, A. Ionescu, S. Holmes, C.H.W. Barnes, A.B. Domínguez, O.A. Quispe, J.C. González, S. Milana, M. Barbone, A.C. Ferrari, H. Ramos, Y. Majima, Characterization of Ni thin films following thermal oxidation in air, J. Vac. Sci. Technol. B 32 (2014) 051808. http://dx.doi.org/10.1116/1.4895846.
[33] G.-X. Zhu, X.-W. Wei, S. Jiang, A facile route to carbon-coated nickel-based metal nanoparticles, J. Mater. Chem. 17 (2007) 2301–2306. http://dx.doi.org/10.1039/B615942G.
[34] J.-H. Hwang, V.P. Dravid, M.H. Teng, J.J. Host, B.R. Elliott, D.L. Johnson, T.O. Mason, Magnetic Properties of Graphitically Encapsulated Nickel Nanocrystals, J. Mater. Res. 12 (1997) 1076–1082. http://dx.doi.org/10.1557/JMR.1997.0150.
[35] D. Kumar, S.J. Pennycook, A. Lupini, G. Duscher, A. Tiwari, J. Narayan, Synthesis and atomic-level characterization of Ni nanoparticles in Al_2O_3 matrix, Appl. Phys. Lett. 81 (2002) 4204–4206. http://dx.doi.org/10.1063/1.1525052.
[36] EC, Regulation No. 1907/2006 of the European Parliament and of the Council of 18 December 2006. Concerning the Registration, Evaluation, Authorisation and Restriction of Chemicals (REACH), in: Official Journal of the European Union, L396/1-849, European Commission, Brussels, Belgium, 2006. ⟨http://data.europa.eu/eli/reg/2006/1907/2014-04-10⟩.
[37] EC, Regulation No. 1272/2008 of the European Parliament and of the Council of 16 December 2008 on classification, labelling and packaging (CLP) of substances and mixtures, amending and repealing Directives 67/548/EEC and 1999/45/EC, and amending Regulation No. 1907/2006, in: Official Journal of the European Union, L 353, European Commission, Brussels, Belgium, 2008. ⟨http://data.europa.eu/eli/reg/2008/1272/oj⟩.
[38] OECD 202, Guideline 202 for the Testing of Chemicals, Daphnia sp. Acute Immobilisation Test. Organisation for Economic Co-operation and Development, Paris, France. 2004. ⟨http://doi.org/10.1787/20745761⟩
[39] OECD 201, Guideline 201 for the Testing of Chemicals, Alga, Growth Inhibition Test. Organisation for Economic Cooperation and Development, Paris, France. 2011. ⟨http://doi.org/10.1787/20745761⟩
[40] A. Kahru, H.-C. Dubourguier, From ecotoxicology to nanoecotoxicology, Toxicology 269 (2010) 105–119. http://dx.doi.org/10.1016/j.tox.2009.08.016.
[41] A.A. Qureshi, R.N. Coleman, J.H. Paran, Evaluation and refinement of the Microtox test for use in toxicity screening, in: D. Liu, B.J. Dutka (Eds.), Toxicity Screening Procedures Using BacterialSystems, Marcel Dekker Inc., New York and Basel, 1984, pp. 1–22.
[42] S.K. Sankaramanachi, S.R. Qasim, Metal toxicity evaluation using bioassay and microtox™, Int. J. Environ. Stud. 56 (1999) 187–199. http://dx.doi.org/10.1080/00207239908711199.
[43] S. Käosaar, A. Kahru, P. Mantecca, K. Kasemets, Profiling of the toxicity mechanisms of coated and uncoated silver nanoparticles to yeast Saccharomyces cerevisiae BY4741 using a set of its 9 single-gene deletion mutants defective in oxidative stress response, cell wall or membrane integrity and endocytosis, Toxicol. Vitr. 35 (2016) 149–162. http://dx.doi.org/10.1016/j.tiv.2016.05.018.
[44] V.J. Cid, A. Duran, F. del Rey, M.P. Snyder, C. Nombela, M. Sanchez, Molecular basis of cell integrity and morphogenesis in Saccharomyces cerevisiae, Microbiol. Rev. 59 (1995) 345–386 (0146-0749/95/$04.0010).